Operational Research
https://doi.org/10.1007/s12351-022-00717-x

ORIGINAL PAPER

Parameter analysis for sigmoid and hyperbolic transfer functions of fuzzy cognitive maps

Themistoklis Koutsellis[1] · Georgios Xexakis[2] · Konstantinos Koasidis[1] · Alexandros Nikas[1] · Haris Doukas[1]

Received: 16 October 2021 / Revised: 6 April 2022 / Accepted: 3 May 2022

Abstract

Fuzzy cognitive maps (FCM) have recently gained ground in many engineering applications, mainly because they allow stakeholder engagement in reduced-form complex systems representation and modelling. They provide a pictorial form of systems, consisting of nodes (concepts) and node interconnections (weights), and perform system simulations for various input combinations. Due to their simplicity and quasi-quantitative nature, they can be easily used with and by non-experts. However, these features come with the price of ambiguity in output: recent literature indicates that changes in selected FCM parameters yield considerably different outcomes. Furthermore, it is not a priori known whether an FCM simulation would reach a fixed, unique final state (fixed point). There are cases where infinite, chaotic, or cyclic behaviour (non-convergence) hinders the inference process, and literature shows that the primary culprit lies in a parameter determining the steepness of the most common transfer functions, which determine the state vector of the system during FCM simulations. To address ambiguity in FCM outcomes, we propose a certain range for the value of this parameter, λ, which is dependent on the FCM layout, for the case of the log-sigmoid and hyperbolic tangent transfer functions. The analysis of this paper is illustrated through a novel software application, *In-Cognitive*, which allows non-experts to define the FCM layout via a Graphical User Interface and then perform FCM simulations given various inputs. The proposed methodology and developed software are validated against a real-world energy policy-related problem in Greece, drawn from the literature.

Keywords Fuzzy cognitive maps · Mental modelling · Transfer function · Parameter selection · Decision making · Participatory modelling

✉ Konstantinos Koasidis
kkoasidis@epu.ntua.gr

[1] Decision Support Systems Laboratory, School of Electrical and Computer Engineering, National Technical University of Athens, Iroon Politechniou 9, 157 80 Athens, Greece

[2] HOLISTIC P.C., Mesogeion Avenue 507, 153 43 Athens, Greece

Published online: 29 May 2022

Mathematics Subject Classification 90C70

1 Introduction

Fuzzy cognitive maps (FCMs) (Kosko 1986) have been used to model systems in many scientific areas, such as in social and political science (Craiger and Coovert 1994; Tsadiras and Kouskouvelis 2005; Axelrod 2015) as well as in economics (Koulouriotis et al. 2001; Carvalho and Tomé 2004; Koulouriotis 2004; Penn et al. 2013; Azevedo and Ferreira 2019). They have also been used in the presentation of social scientific knowledge and description in various decision-making methods (Zhang et al. 1989, 1992; Georgopoulos et al. 2003). Other notable applications include geographical information systems (Liu and Satur 1999; Satur and Liu 1999b, a), pattern-recognition applications (Papakostas et al. 2006, 2008), numerical and linguistic prediction of time-series functions (Silva 1995; Stach et al. 2008), technological (Stylios and Groumpos 2004), industrial (Abbaspour Onari and Jahangoshai Rezaee 2020; Markaki and Askounis 2021) and medical applications (Froelich et al. 2012; Amirkhani et al. 2017, 2018; Apostolopoulos et al. 2017; Bevilacqua et al. 2018; Puerto et al. 2019).

Several other studies have also employed FCMs in environmental and ecological problems (Hobbs et al. 2002; Fons et al. 2004; Xirogiannis et al. 2004; Çelik et al. 2005; Mendoza and Prabhu 2006; Kok 2009; Ceccato 2012; Soler et al. 2012; Cakmak et al. 2013; Gray et al. 2014) or energy policy and efficiency projects (Ghaderi et al. 2012; Kyriakarakos et al. 2012; Huang et al. 2013; Reckien 2014; Hsueh 2015; Karavas et al. 2015; Amer et al. 2016; Olazabal and Pascual 2016; Nikas and Doukas 2016; Nikas et al. 2020, 2019; Antosiewicz et al. 2020; Doukas and Nikas 2020). As a policy support tool, FCMs have particularly gained ground in such energy and climate policy applications, partly due to stakeholders encountering difficulties in understanding, or being excluded from, state-of-the-art policy support frameworks, like energy- and climate-economic modelling tools (Nikas and Doukas 2016). Due to limited model complexity and reliance on quantitative data, FCMs have proliferated as a policy support tool, especially at the local level, allowing policymakers to reflect their understanding of a problem domain in a structured manner and act based on it (Özesmi and Özesmi 2004). They have also been proposed as an effective way to bridge the science-policy gap and engage stakeholders in environmental modelling processes (van Vliet et al. 2010).

Broadly speaking, however, the simplicity and attractiveness of FCMs across application areas and domains lies in their ability to capture the perception of a system in graphical representations consisting of concepts (nodes) and interconnections (weights) among these nodes, which are characterised by transfer functions determining the state vector of the system in simulation (Tsadiras 2008). However, the topology of nodes and weights, on the one hand, and the transfer function, on the other, are formulated differently: the former are typically defined by the non-expert decision makers (stakeholders) of the case study, while the latter are selected by the analysts. In essence, like stakeholders, the analysts are required to take decisions, which are both relevant to the analysis and critical to its results.

However, despite the plethora of applications, the FCM theory is still inconsistently applied in the literature (Felix et al. 2019). Notably, there seems not to exist a common ground among researchers regarding one of its core features, the type of transfer function used to drive simulations. Various monotonic functions have been used in literature, such as step, sigmoidal, ramp, and linear functions (e.g. Hobbs et al. 2002; Mendoza and Prabhu 2006) and (Soler et al. 2012)), with each one potentially yielding markedly different results. This diversity in FCM outcomes imposes barriers to the final inference procedure. In the absence of common criteria on selecting the transfer function, analysts should carefully justify their choice based on the physical interpretation of each application, which however is not common practice (Nápoles et al. 2018).

In this paper, we propose the use of two transfer functions, namely the log-normal (sigmoid) and hyperbolic tangent functions. We also introduce a criterion to define their parameter λ—i.e., their steepness—toward standardising the selection of the FCM transfer function. The observations and analysis in this study build on previous studies (Boutalis et al. 2008; Kottas et al. 2010; Lee and Kwon 2010; Knight et al. 2014; Harmati and Kóczy 2018; Harmati et al. 2018), which provided bounds for parameter λ. Depending on the λ value, the sigmoid and hyperbolic tangent functions yield a unique final state of nodes for a given set of input values (i.e., a fixed state vector). However, by providing a domain of parameter λ, they only restrict λ values so they do not yield chaotic, ambiguous FCM responses. The selection of parameter λ is thus still subject to the subjective selection of the analyst within the provided bounds.

Despite providing final node values with clear ordering, the linear transfer function suffers from the undesired condition of chaotic final states (Knight et al. 2014). Additionally, although the sigmoid and hyperbolic tangent functions—given parameters λ within specific bounds provided in the literature—do not exhibit such behaviour, they often result in final node values close to one another, thereby hindering clear inference. To tackle these barriers, we propose an improved version of sigmoid and hyperbolic tangent transfer functions, which is active within an *almost-linear region*. We illustrate this methodology through a Python web software application "In-Cognitive" that we developed in the context of this study. This novel application features a user-friendly Graphical User Interface (GUI) that allows various stakeholders to define the FCM layout (e.g., nodes, weight interconnections, input/initial state vector, etc.), and execute scenario simulations before reaching a final state vector. The value of parameter λ is calculated endogenously, based on the proposed analysis.

Section 2 provides a theoretical background (notations and definition) of fuzzy cognitive mapping. In Sect. 3, we provide an FCM analysis without considering input nodes (all nodes may change throughout the simulation iterations): we first present and discuss the state-of-the-art bounds of parameter λ, before introducing a framework to define bounds/value of λ parameter. Section 4 performs similar analysis for the case of FCMs with given input nodes that remain steady and unaffected by other nodes throughout the simulation. The "In-Cognitive" software application is presented in Sect. 5 and then validated in Sect. 6 in a case

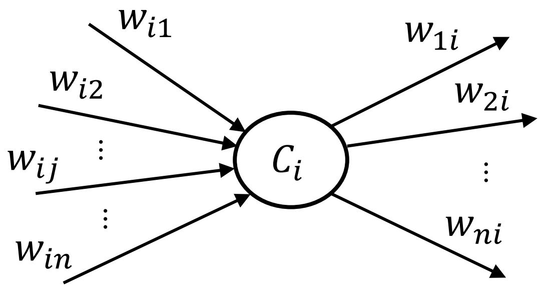

Fig. 1 A node and its interconnections

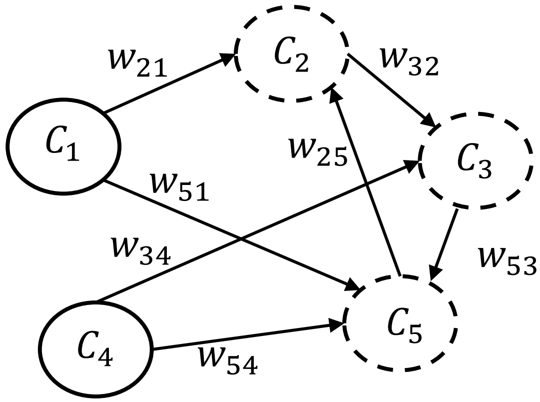

Fig. 2 Example of a small FCM, with steady nodes (C_1 and C_4) represented by solid-border circles and intermediate nodes (C_2, C_3, and C_5) represented by dotted-border circles

study drawn from the literature. Section 7 finally concludes the research, highlighting key takeaways and discussing prospects.

2 FCM background and layout notations

An FCM consists of n concepts (nodes), $C_i : i = 1, 2, \ldots, n$, linked to one another through a weight, w_{ij}, which describes the degree of influence of C_j over C_i within $[-1, 1]$. When $w_{ij} < 0$ (negative causality), C_i decreases for an increase in C_j. When $w_{ij} > 0$ (positive causality), C_i increases for an increase in C_j. Finally, when $w_{ij} = 0$ there is no relationship (nor adjacency) between C_j and C_i. Figure 1 illustrates how node C_i is connected through weights with all the other nodes.

Input or *steady* nodes, steady nodes hereafter, influence but are not influenced by other nodes (i.e., they have outbound but no inbound links). The nodes which are neither steady nodes nor output nodes are called *intermediate* nodes. In Fig. 2, an FCM of 5 nodes is presented: nodes C_1 and C_4 (solid circles) are steady nodes, while nodes C_2,

C_3 and C_5 (dotted circles) are intermediate nodes. For a real-world example, the reader is referred to Sect. 6.

The matrix consisting of all FCM weights w_{ij} is called the weight matrix, $\boldsymbol{W}$. Equation (1) shows the weight matrix of the FCM illustrated in Fig. 2.

$$\boldsymbol{W} = \begin{bmatrix} w_{1,1} & w_{1,2} & w_{1,3} & w_{1,4} & w_{1,5} \\ w_{2,1} & w_{2,2} & w_{2,3} & w_{2,4} & w_{2,5} \\ w_{3,1} & w_{3,2} & w_{3,3} & w_{3,4} & w_{3,5} \\ w_{4,1} & w_{4,2} & w_{4,3} & w_{4,4} & w_{4,5} \\ w_{5,1} & w_{5,2} & w_{5,3} & w_{5,4} & w_{5,5} \end{bmatrix} = \begin{bmatrix} 0 & 0 & 0 & 0 & 0 \\ w_{2,1} & 0 & 0 & 0 & w_{2,5} \\ 0 & w_{3,2} & 0 & w_{3,4} & 0 \\ 0 & 0 & 0 & 0 & 0 \\ w_{5,1} & 0 & w_{5,3} & w_{5,4} & 0 \end{bmatrix}. \tag{1}$$

3 FCM equilibrium analysis with no steady nodes

To analyse FCM outcomes, we express node interactions using a mathematical formulation that should be iterative through time. If A_i^k is the value of node i at time instance k, the iterative interconnection expression for each node is

$$A_i^{k+1} = f\left(\sum_{j=1, i\neq i}^{n} \left(w_{ij} A_j^k + d_i A_i^k \right) \right), \tag{2}$$

where $f(\cdot)$ is the transfer function and d_i the feedback coefficient $\in [0, 1]$. The latter indicates the dependency of node C_i on its starting value in each iteration. The transfer function could be any function. However, to avoid chaotic FCM behaviours, the transfer function values should be bounded. Usually, the *log-sigmoid* and *hyperbolic tangent* functions are used. The values of the former span within [0,1] and of the latter within [− 1,1]. The general form of the log-sigmoid function is

$$f_s = \frac{1}{1 + exp(-\lambda x)} \tag{3}$$

whereas the corresponding one of the hyperbolic tangent is

$$f_h = \frac{exp(\lambda x) - \exp(-\lambda x)}{\exp(\lambda x) + exp(-\lambda x)} = \frac{exp(2\lambda x) - 1}{exp(2\lambda x) + 1}. \tag{4}$$

As discussed in (Knight et al. 2014), the selection of the transfer function should be justified based on the given application and, therefore, there is no standard criterion to yield the best fitted transfer function; Knight et al. also show that different types of transfer functions yield different FCM final states and thus different inferences. To tackle this issue, Knight et al. proposed the execution of various simulations, with each one having different transfer functions. They then compared results to identify common patterns: nodes, whose final values are relatively high (low) for all executions are considered the most (least) important FCM concepts.

3.1 State-of-the-art bounds of parameter λ of transfer functions

Different types of transfer functions yield different inferences for the iterative function of Eq. (2)—similarly, different λ parameters of the same transfer function (see Eqs. (3) and (4)) may yield different FCM final states and therefore different inferences. Some of the various final states of Eq. (2) might be chaotic, infinite, or periodic (Knight et al. 2014). These states are not fit for any kind of inferences. Therefore, it is necessary to ensure the FCM converges and explore whether a given layout can be stabilised around a final steady state after several iterations of Eq. (2).

Under certain conditions and a given combination of (a) the weight matrix, (b) the number of nodes, and (c) the parameters of the transfer function, it is possible to reach a final, unique fixed vector regardless of the initial values $A_i^0, \forall i \in [0, n]$. It should be noted that, for any of these combinations, the final state is not necessarily the same.

It should be noted that, in previous research (Boutalis et al. 2008; Kottas et al. 2010; Lee and Kwon 2010; Knight et al. 2014; Harmati and Kóczy 2018; Harmati et al. 2018), the authors provided conditions under which the existence and uniqueness of solutions of concept values (see Eq. (2)) are guaranteed. In Knight et al. (2014), the authors provided a maximum bound of λ parameter for the log-sigmoid transfer function (see Eq. (3)), regardless of the structure and contents of the weight matrix; they also showed that, when the FCM is equipped with a step function (i.e., the limit state of log-sigmoid function when $\lambda \to \infty$), the uniqueness and existence of a fixed solution is not guaranteed as well as that, as the examined FCM grows in size ($n \to \infty$, where n the number of FCM nodes), the λ parameter to guarantee the existence and the uniqueness of a final fixed solution gets smaller ($\lambda \to 0$). However, the provided upper bounds of λ parameter were strict enough, rendering unnecessary the consideration of the layout of a given FCM (i.e., the weigh matrix). In Kottas et al. (2010), the authors provided a less strict upper bound conditions, under which there is a fixed-point solution when $\lambda = 1$, for both Eqs. (3) and (4), depending also on the weight matrix/structure. Consequently, the conditions discussed in Knight et al (2014) are less restrictive in case $\lambda = 1$. In Harmati et al. (2018), the authors extended the results of Kottas et al. (2010) for all $\lambda > 0$ and finally reached a bound of λ for all log-sigmoid and hyperbolic tangent-equipped FCM implementations.

In the case of the log-sigmoid transfer function, the bound guaranteeing the existence and uniqueness of FCM final state is found to be (Harmati et al. 2018):

$$\lambda_s < \lambda_s' = \frac{4}{\|\boldsymbol{W}\|_F}. \tag{5}$$

Whilst, in the case of the hyperbolic tangent transfer function, the bound is:

$$\lambda_h < \lambda_h' = \frac{1}{\|\boldsymbol{W}\|_F}, \tag{6}$$

where $\boldsymbol{W}$ is the weight matrix and $\|\cdot\|_F$ the Frobenius norm, such that:

$$\|\mathbf{W}\|_{\mathrm{F}} = \sqrt{\sum_{i=1}^{n}\sum_{j=1}^{n}\left(w_{ij}^{2}\right)}. \tag{7}$$

It should be noted that the above conditions are sufficient, but not necessary for an FCM to have one and only one fixed point for a given parameter λ: there could be cases where an FCM has a unique fixed-point solution if λ is greater than the above upper bounds (see Eqs. (5) and (6)).

Lee and Kwon (2010) reached similar conclusions for the log-sigmoid transfer function, by using a different approach (Lyapunov criteria).

3.2 Remarks on transfer functions

Among many transfer functions, the linear function—more specifically the identity function—yields lucid inferences, because the distance among outcomes is clearer than other transfer functions (Knight et al. 2014). Based on the structure of Eq. (2), the linear function features no distortion during the calculation of A_i^{k+1} from previous iterative values A_j^k. The value of the transfer function is always proportional to the argument of Eq. (2) through all iterations. This property of linear functions gives room to lucid inferences; the distance among the final node values is sufficient to distinguish each node final state from the others. However, the linear transfer function comes with certain caveats. Often, during iterations, the A_i^{k+1} values are constantly increasing (decreasing) reaching infinite (minus infinite) values. Despite FCMs equipped with linear transfer functions exhibiting a closer-to-reality increment (decrement), the above extreme case behaviour is restrictive for the execution of the iterative procedure (Eq. (2)). For this reason, the analysts tend to impose restrictions on A_i^{k+1} values by using bounded transfer functions—i.e., the log-sigmoid and hyperbolic tangent function. Both are odd functions around the $y = 0.5$ and $y = 0$ axis, respectively, and exhibit an *almost-linear* behaviour in a region close to these axes. This linearity gives them resemblance to a linear transfer function for a sufficient interval. The non-linear regions on the tails of these functions are used to represent the large A_j^{k+1} values. The $y = 0$ and $y = 1$ bounds ($y \pm 1$ bounds) are used to represent the infinite (or close to infinity) A_j^{k+1} values for the case of the log-sigmoid (hyperbolic tangent) transfer function (see Fig. 3). The heavy curved regions close to these bounds are mainly responsible for the distortion (non-proportionality) of A_j^{k+1} values; arguments close to infinite tend to map to almost the same A_j^{k+1} values (i.e., no sufficient distance among nodes' final values).

However, bounded transfer functions exhibit shortcomings as well. Not only do the non-linear regions introduce distortion, but the existence of bounds ($y = 0$ and $y = 1$, or $y \pm 1$) could yield final states that are either chaotic or limit cycles (i.e., a period function of A_i). This could happen when the x_i^k arguments of Eq. (2)

$$x_i^{k+1} = \sum_{j=1, i\neq i}^{n}\left(w_{ij}A_j^k + d_iA_i^k\right), \tag{8}$$

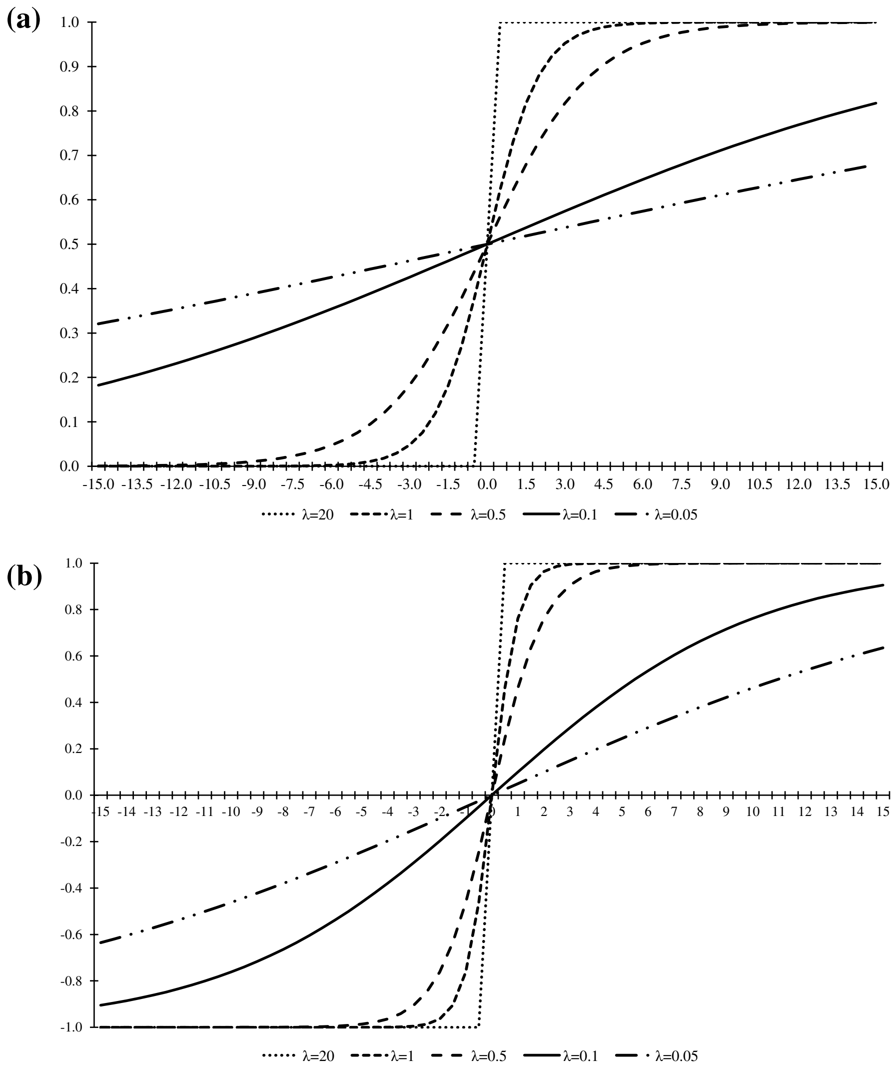

Fig. 3 Plot of **a** a log-sigmoid function and **b** a hyperbolic tangent function

exhibit prolonged stay in the area where $f_s \to +1$ or $f_s \to 0$ (log-sigmoid case), or $f_h \to \pm 1$ (hyperbolic tangent case) during the iterative procedure of Eq. (2). In this case, it is more likely for the FCM simulation to conclude to a state where all final A_i values are close to 0 or 1 (log-sigmoid) or ± 1 (hyperbolic tangent) making the ordering of final A_i values obscure. From Fig. 3, we can conclude that this undesired behaviour happens when parameter λ exhibits large values (i.e., f is almost a step function). Knight et al. (2014) reached the same conclusion by using a different approach. Similarly, another case yielding cyclic behaviour happens when the x_i^k values are perpetually changing sign through iterations and parameter λ is simultaneously large enough (i.e., the transfer function is almost a step function). In that case, the A_i values are more likely to oscillate with an amplitude having extreme values close to the bounds of the transfer function. Such oscillations in node values are almost chaotic and insufficient for inferences. As a rule of thumb, the FCM analyst should therefore avoid large values of the λ parameter.

Another undesirable condition occurs when parameter λ is too small (almost zero). When $\lambda \to 0$, the transfer function is almost flat (see Fig. 3) in all ranges of x_i^k values and, therefore, all A_i values conclude to almost the same value. This state is stable; however, it cannot reach a conclusion because there is no lucid ordering among A_i values. Concluding, FCM analysts should avoid both small and large values of parameter λ. Below we propose an upper bound of parameter λ based on the above remarks. These bounds can thereafter be combined with the bounds of Eqs. (5) and (6).

3.3 Proposed bounds for parameter λ

The proposed methodology refers to FCMs equipped with the log-sigmoid or hyperbolic tangent transfer function. It is based on the conclusion that $\lambda \to 0$ and $\lambda \to \infty$ are two undesired regions of parameter λ and the assertion that linear transfer functions are preferable, if they do not yield chaotic, cyclic, or infinite final states (see Sect. 3.2). The main idea behind the proposed methodology is that both log-sigmoid and hyperbolic tangent transfer functions have a region that is almost linear (desired region). We provide certain conditions, under which all A_i^{k+1} values fall within that region. These conditions are then used to provide bounds of parameter λ. By operating in the almost linear region, we get a combination of benefits of both linear and bounded transfer functions (see Sect. 3.2); mainly, we avoid the distortion that the curved segments in the tails of the bounded transfer functions introduce (Fig. 4).

However, working in the almost linear region comes at a cost. This region is not as large as the interval between the bounds of the log-sigmoid or hyperbolic tangent function; therefore, the final A_i^{k+1} values are usually close to one another. To avoid this, we propose a normalisation procedure (see Sect. 3.4).

3.3.1 The almost linear region of the log-sigmoid and hyperbolic tangent functions

For the almost linear region to be ‘active’ for all nodes during all FCM iterations, all arguments x_i^k’s (Eq. (8)) must not lie in the region of the transfer function tails. The desired region where x_i^k values lie on is hereafter called ‘almost linear region’ (see Fig. 4); all x values bounded by $-x^*$, $+x^*$, where $f'''(\pm x^*) = 0$, which is where the f'' has local maxima (see Fig. 4). We call $-x^*$ and $+x^*$ "turning points," hereafter.

The third derivative of log-sigmoid (Eq. (3)) is

$$f_s'''(x) = \lambda^2 f_s'(x)\left\{\left(1 - f_s(x)\right)\left(1 - 2f_s(x)\right) - f_s(x)\left(1 - 2f_s(x)\right) - 2f_s(x)\left(1 - f_s(x)\right)\right\}. \tag{9}$$

The third derivative of hyperbolic tangent (Eq. (4)) is:

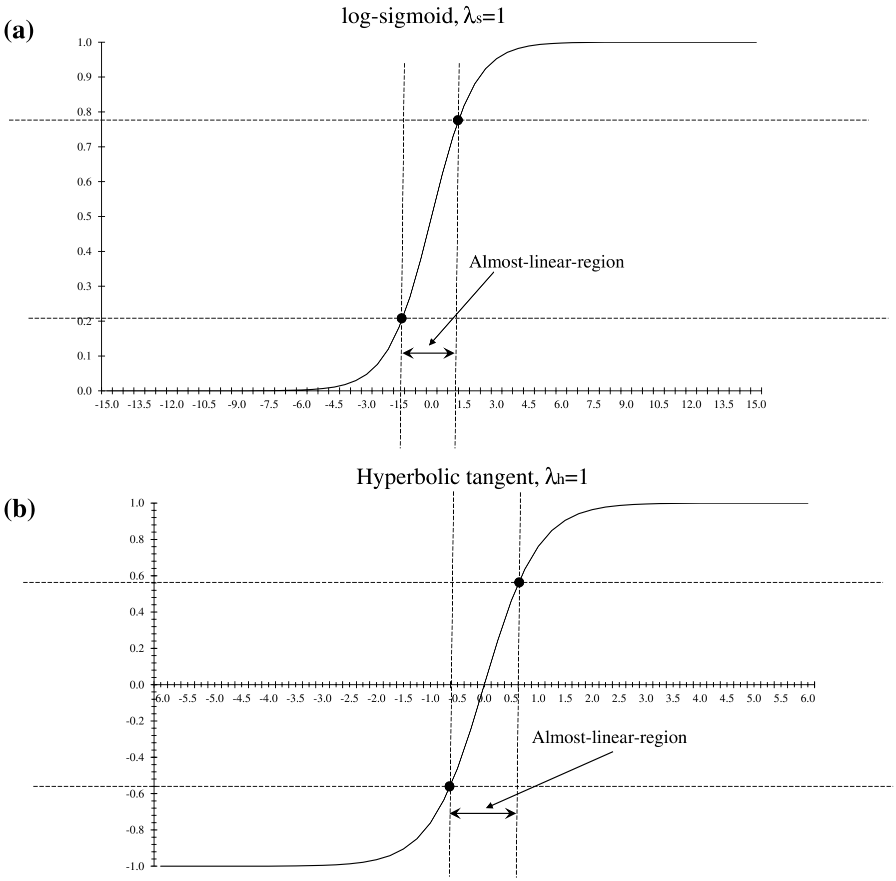

Fig. 4 The almost linear region of **a** a log-sigmoid function and **b** a hyperbolic tangent function

$$f_h'''(x) = -2\lambda f_h''(x)\left(f_h(x) + f_h''(x)\right). \tag{10}$$

The λ parameter is always positive, as well as $f_s'(x)$ (Kottas et al. 2010). Then, after equating the $\{\cdot\}$ factor of Eq. (9) with zero, we conclude to $\left(f_s(x)\right)^2 - f_s(x) + (1/8) = 0$, which is true if $f_s(x) \approx 0.789$ or $f_s(x) \approx 0.211$. Therefore, $0.211 \leq f_s(x) \leq 0.789$ (see Fig. 4a). After using Eq. (3), we finally get $0.211 \leq \frac{1}{1+exp\left(-\lambda_s x\right)} \leq 0.789$, which is equivalent to:

$$-1.317 \leq \lambda_s \cdot x \leq 1.317, \tag{11}$$

where λ_s is parameter λ of the log-sigmoid transfer function.

Similarly, from Eq. (10) we get that

$$-0.658 \leq \lambda_h \cdot x \leq 0.658, \tag{12}$$

where λ_h is parameter λ of the hyperbolic tangent transfer function.

The almost linear region is odd with respect to the $x = 0$ axis and parameter λ is always positive; therefore, we can rewrite Eqs. (11) and (12) as

$$0 \leq \lambda_s \cdot |x| \leq 1.317,\ \forall x \tag{13}$$

and

$$0 \leq \lambda_h \cdot |x| \leq 0.658,\ \forall x. \tag{14}$$

3.3.2 Bounds of parameter λ witch quarantine that the almost linear region is always "active"

Equations (13) and (14) indicate that all absolute argument values multiplied by parameter λ (i.e., $\lambda \cdot \left| x_i^k \right|$) should lie in intervals $[0, 1.317]$ or $[0, 0.658]$, respectively. This is satisfied if the largest argument $\lambda \cdot \left| x_i^k \right|_{max}$ is smaller or equal to the upper bound of each interval. Substituting the argument of Eq. (8) to $\left| x_i^k \right|_{max}$ we get $\left| \sum_{j=1, i \neq i}^{n} \left(w_{ij} A_j^k + d_i A_i^k \right) \right|_{max}$.

When the transfer function is log-sigmoid, all state values are positive, that is $0 < A_j^k < 1$. If we need to restrict the A_j^k values to the "almost linear region" (see Fig. 4), then $0.211 \leq A_j^k \leq 0.789$. In contrast, the w_{ij} values could be positive or negative. Given the maximum values of A_j^k and w'_{ij} values for a specific i node, the maximum value $\left| x_i^k \right|$ is equal to

$$\left| x_i^k \right| \Big|_{max} = max\left(\left| 0.211 \cdot \sum_{i=1}^{p} w_{ij}^{+} + 0.789 \cdot \sum_{i=1}^{q} w_{ij}^{-} \right|, \left| 0.211 \cdot \sum_{i=1}^{p} w_{ij}^{-} + 0.789 \cdot \sum_{i=1}^{q} w_{ij}^{+} \right| \right) \tag{15}$$

where w_{ij}^{+}'s and w_{ij}^{-}'s are all positive and negative input weights, respectively, which end up to the ith node.

We define as *s-norm* of matrix $\boldsymbol{W}$, $\|\boldsymbol{W}\|_s$, the following

$$\|\boldsymbol{W}\|_s = \max_i \left(\left| x_i^k \right| \Big|_{max} \right). \tag{16}$$

From Eq. (16) we can see that the maximum value the absolute arguments $\left| x_i^k \right|$ could get is

$$|x|\,|_{max} = \|\boldsymbol{W}\|_s. \tag{17}$$

Therefore, from Eqs. (13) and (17) we finally conclude

$$\lambda_s \leq \lambda_s^* = \frac{1.317}{\|\boldsymbol{W}\|_s}. \tag{18}$$

For an FCM equipped with the hyperbolic tangent transfer function, the maximum value the absolute arguments $\left| x_i^k \right|$ could get through all iterations is different because $-1 < A_j^k < 1$. The A_j^k will fall in the 'almost linear region' when

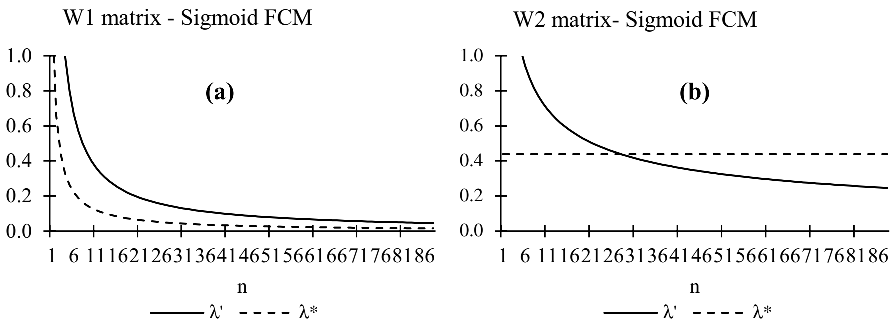

Fig. 5 Comparison of lambda parameter bounds for two different weight matrices (log-sigmoid transfer function)

$-0.577 \leq A_j^k \leq 0.577$. Therefore, the possible maximum value for node C_i could be achieved if all w_{ij}^{+} are multiplied by $+0.577$ (-0.577) and all w_{ij}^{-} by -0.577 ($+0.577$). Equivalently, the maximum value of $\left|x_i^k\right|$ could be achieved when $\left|x_i^k\right| = 0.577 \cdot \left(\sum_{\iota=1}^{n} \left|w_{ij}\right|\right)$. The latter factor is equal to the infinite norm of the weight matrix, $\boldsymbol{W}$, which is equal to the maximum absolute row sum of $\boldsymbol{W}$. Therefore,

$$|x||_{max} = 0.577 \cdot \|\boldsymbol{W}\|_{\infty}, \tag{19}$$

where $\|\boldsymbol{W}\|_{\infty} = \max_i \sum_{j=1}^{n} \left|w_{ij}\right|$, the infinite norm of $\boldsymbol{W}$ matrix. From Eq. (14) we conclude

$$\lambda_h \leq \lambda_h^* = \frac{1.14}{\|\boldsymbol{W}\|_{\infty}}. \tag{20}$$

The ordering among parameters λ_s', λ_s^* and λ_h', λ_h^* is not constant for all applications. As such, we cannot a priori conclude to the existence and uniqueness of the FCM fixed-point if $\lambda < \lambda_s^*$ or $\lambda < \lambda_h^*$. Figure 5 illustrates the bounds λ_s' and λ_s^* for weight matrices $\boldsymbol{W}_{1_{(n\times n)}} = \boldsymbol{J_n}$ and $\boldsymbol{W}_{2_{(n\times n)}}$, where $\boldsymbol{W}_1$ is a matrix of ones and $\boldsymbol{W}_2$ is a square matrix having three elements per row, all of which are equal to one and aligned around its diagonal. $\boldsymbol{W}_2$ could represent an FCM whose nodes are only connected with their three adjacent nodes ($\boldsymbol{W}_{2_{(1\times1)}}$ and $\boldsymbol{W}_{2_{(2\times2)}}$ are equal to matrices of ones because their size is smaller than three). From Fig. 5 it can be shown that the ordering of bounds λ_s' and λ_s^* changes depending on the size (the number of nodes) and type (e.g., $\boldsymbol{W}_1$ or $\boldsymbol{W}_2$) of the weight matrix. Similar conclusions can be drawn for λ_h' and λ_h^*.

Based on the above remarks, when λ_s' (λ_h') is greater than $\lambda_s^*(\lambda_h^*)$, the FCM analysts should choose the $\lambda_s^*(\lambda_h^*)$. By doing so, they can guarantee that there would be a fixed final point due to $\lambda < \lambda_s'$ ($\lambda < \lambda_h'$) and that this fixed point would consist of A_i values lying in the 'almost linear region' of the transfer function. On the other hand, if $\lambda_s^*(\lambda_h^*)$ is greater than λ_s' (λ_h'), the λ_s' (λ_h') should be preferred to guarantee that there would be a unique fixed point. These remarks can be formulated as follows:

$$\lambda_s < min\left(\lambda_s', \lambda_s^*\right) \tag{21}$$

for the log-sigmoid transfer function, and

$$\lambda_h < min\left(\lambda_h', \lambda_h^*\right) \tag{22}$$

for the hyperbolic tangent transfer function.

Once the final bound is estimated (Eq. (21) or Eq. (22)), we should choose a parameter λ that is as close to the final bound as possible, because parameter λ must not get extremely low values, $\lambda \to 0$ (see Sect. 3.2). This value is the infimum value of bounds in Eq. (21) and Eq. (22). For the sake of simplicity, we propose as close to infimum λ value, which is derived after rounding the final bound of Eq. (21) or Eq. (22) at the third decimal digit.

3.4 Normalisation of final state values

The proposed λ bounds squash all concept values during all iterations within $[0.211, 0.789]$ and $[-0.577, 0.577]$ for log-sigmoid and hyperbolic tangent transfer functions, respectively. This may end up to final output values close to one another. Consequently, the relative distance among these values might be unclear. To return to the $[0, 1]$ or $[-1, 1]$ interval for log-sigmoid and hyperbolic tangent, respectively (normalised intervals, hereafter), we need to multiply all these values with a factor so that the A_j^k values are within these normalised intervals.

All concept values, during all iterations, lie in the almost linear region and are, therefore, within the following intervals:

$$0.211 \leq A_j^k \leq 0.789 \tag{23}$$

and

$$-0.577 \leq A_j^k \leq 0.577, \tag{24}$$

for log-sigmoid and hyperbolic tangent, respectively. For the case of a log-sigmoid FCM, to normalise A_j^k we should express them in terms of the $y = 0.5$ line. Recall that the log-sigmoid function is an odd function with respect to $y = 0.5$. After subtracting 0.5 from Eq. (23) we get $-0.289 \leq A_j^k - 0.5 \leq 0.289$. Equivalently, $\frac{-0.289}{2\cdot 0.289} = -0.5 \leq \frac{A_j^k - 0.5}{2\cdot 0.289} \leq \frac{0.289}{2\cdot 0.289} = 0.5 \Leftrightarrow 0 \leq \frac{A_j^k - 0.5}{2\cdot 0.289} + 0.5 \leq 1$. We conclude:

$$0 \leq \frac{A_j^k - 0.211}{0.578} \leq 1. \tag{25}$$

Therefore, to normalise the final values of all FCM nodes, we need to subtract -0.211 for any of them and then divide them with 0.578.

Similarly, for hyperbolic tangent FCMs, the necessary transformation to normalise the final values of FCM nodes is the multiplication with 1.733:

$$-1 \leq 1.733 \cdot A_j^k \leq 1. \tag{26}$$

4 FCM equilibrium analysis with steady nodes

In Sect. 3, we presented conditions, under which an FCM with no input/steady nodes has a unique solution ($\lambda < \lambda_s'$) consisting of final A_i values distinct enough ($\lambda < \lambda_s^*$) to yield lucid inferences. In case of FCM with steady nodes though, which is the case for scenario analysis (Nikas et al. 2019, 2020; Antosiewicz et al. 2020) the unique equilibrium does not depend solely on the weight matrix and parameter λ, as it does in the case of FCMs with no input nodes; it also depends on the values of the steady nodes (external excitations). Therefore, we can achieve a variation of equilibria/responses by changing the excitation of steady nodes and simultaneously reassuring that we will not get a chaotic final state if we choose certain values of parameter λ similarly to Eqs. (21) and (22). To do so, we must express parameter λ with respect to the weight set of the non-steady nodes (Kottas et al. 2010).

4.1 Bounds of λ parameter when there are steady/input FCM nodes

Based on Kottas et al. (2010), the existence of equilibrium is guaranteed if Eqs. (5) and (6) are valid for the weight set of the non-steady nodes. First, we need to reconstruct the extended weight matrix, $\boldsymbol{W}$, so that the first rows correspond to the steady-nodes and the end rows to the non-steady nodes. That is

$$\boldsymbol{W} = \begin{bmatrix} w_{11} & 0 & \cdots & 0 & 0 \\ 0 & w_{22} & \cdots & 0 & 0 \\ \vdots & \vdots & \vdots & \vdots & \vdots \\ \hline \multicolumn{5}{c}{\boldsymbol{W}^*} \end{bmatrix} \tag{27}$$

The FCM illustrated in Fig. 2 with

$$\boldsymbol{W} = \begin{bmatrix} 0 & 0 & 0 & 0 & 0 \\ 0 & 0 & 0 & 0 & 0 \\ w_{2,1} & 0 & 0 & 0 & w_{2,5} \\ 0 & w_{3,2} & 0 & w_{3,4} & 0 \\ w_{5,1} & 0 & w_{5,3} & w_{5,4} & 0 \end{bmatrix} \tag{28}$$

has now the following reconstructed extended weight matrix

$$\boldsymbol{W}^* = \begin{bmatrix} w_{2,1} & 0 & 0 & 0 & w_{2,5} \\ 0 & w_{3,2} & 0 & w_{3,4} & 0 \\ w_{5,1} & 0 & w_{5,3} & w_{5,4} & 0 \end{bmatrix}. \tag{29}$$

To identify the conditions, under which an FCM with steady nodes has equilibrium, Kottas et al. (2010) considered the case where $\lambda = 1$. In this research, we propose the corresponding inequality $\forall \lambda \in \mathbb{R}$. The mathematical proof follows similar steps as described in Harmati et al. (2018). Equation (30) corresponds to an FCM equipped with log-sigmoid whereas Eq. (31) with a hyperbolic tangent transfer function.

$$\lambda_s < \lambda'_s = \frac{4}{\|\mathbf{W}\|_{\mathrm{F}}^*}, \tag{30}$$

$$\lambda_h < \lambda'_h = \frac{1}{\|\mathbf{W}\|_{\mathrm{F}}^*}. \tag{31}$$

Similarly, the λ_s^* and λ_h^* bounds, when the FCM has steady nodes, are

$$\lambda_s^* = \frac{1.317}{\|\mathbf{W}\|_s^*}, \tag{32}$$

and

$$\lambda_h^* = \frac{1.14}{\|\mathbf{W}\|_\infty^*}. \tag{33}$$

Finally, as in the case of non-steady nodes, Eqs. (21) and (22) must be satisfied.

As in Sect. 3.3.2, we propose that the final λ would be derived by the final bound of Eq. (21) or Eq. (22) rounded at the third decimal digits.

4.2 Normalisation of final state values when there are steady FCM nodes

The normalisation procedure when there are steady FCM nodes is like the one described in Sect. 3.4. However, it is applied only to the intermediate and output nodes and, for that reason, only the relative distance between the final values of intermediate and output nodes is suitable for inferences. Equivalently, there is no direct relationship between the qualitative values of input and intermediate or output node values. That is, if $A_1 = 0.6$ is the final value of input node C_1 and $A_{10} = 0.6$ that of C_{10}, we cannot conclude that both C_1 and C_{10} exceed the same amount of deviation. Contrary, if, for example, $A_7 = 0.6$ is an intermediate or output node, we can conclude that it exceeds the same amount of variation with the output node C_{10}. The above restriction is applied because the analysis of Sect. 3.3.2 is applied to the

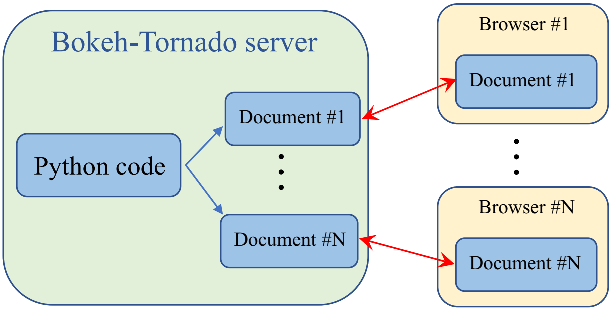

Fig. 6 Description of In-Cognitive Python web application

$\boldsymbol{W}^*$ matrix, which corresponds to the intermediate and output nodes (not the input/steady nodes) or, in other words, only the transfer functions of the intermediate and output nodes perform in the "almost linear region".

5 Software implementation: the "In-Cognitive" tool

There exist several software solutions for FCM design and simulation [see Nikas et al. (2019) and Tsadiras et al. (2021) for detailed accounts]. The In-Cognitive software tool[1] is a web-based interactive application for the creation, visualisation, and simulation of FCMs, featuring the methodology presented in Sects. 3 and 4. It is written in the Python programming language (Python 3.7.3) and based on the Bokeh Python library (Bokeh 2.4.0.). It consists of a client-side web GUI (front-end) and a web server (back-end), with the former exchanging information and queries with Python code/modules stored in the latter. The front-end uses the JavaScript and HTML/CSS technologies to implement the interaction procedure with the end-user (analyst or otherwise). Both JavaScript and HTML/CSS codes are automatically created by the Python Bokeh framework driven by Python scripts. The back-end is built on top of a Tornado Python web framework. In Fig. 6, we briefly illustrate the interaction between the front-end and back-end parts of the In-Cognitive application. As a main functionality, browsers request documents (contents of the web pages) and the server's Python code provides them. The user interacts with the content of documents and ask for services. The document catches these events and afterwards send out feedbacks to the server that listens to these request events.

Figure 7 illustrates the developed GUI. It is divided into two subsections: the (a) FCM editor and display layout, and (b) the simulation outcome subsection. The end-user can easily interact with the FCM editor in order to introduce the FCM layout or edit an existing one and configure the FCM by defining the structure and parameters (i.e., node interconnections, weights, input node values/excitations, transfer function). Parameter λ is automatically calculated based on the analysis in Sects. 3, 4 and, thus, the end-user need not insert any specific value for this parameter. Finally, the end-user can also alter the format (e.g., size, colour, etc.) of the introduced FCM components (e.g., nodes, edges, etc.) to a preferable format and save afterwards the

[1] https://github.com/ThemisKoutsellis/InCognitive

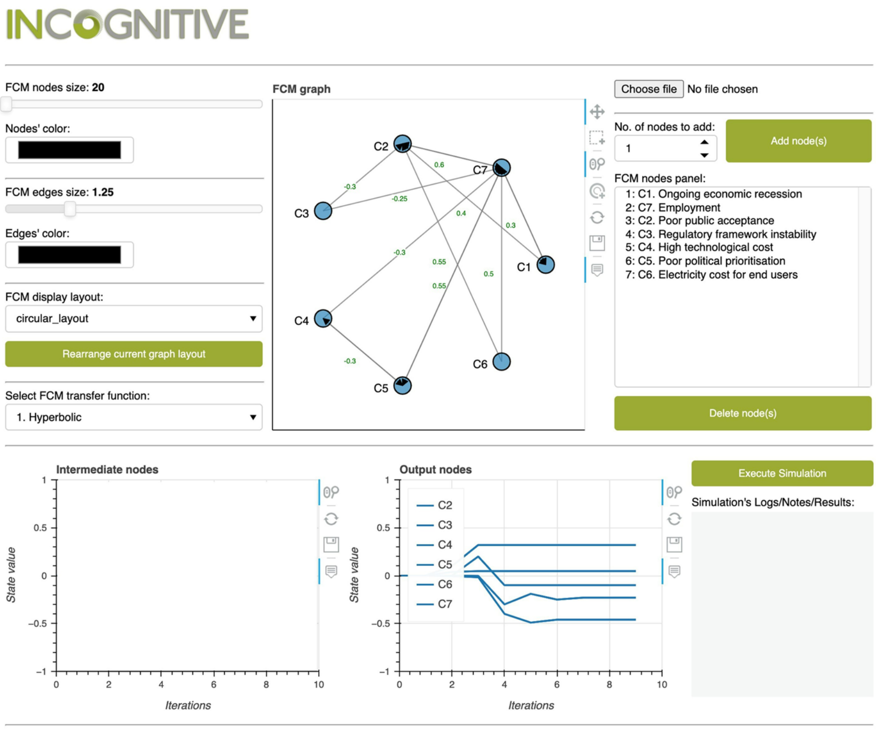

Fig. 7 The In-Cognitive GUI

figure of the introduced FCM layout. In the GUI subsection (b), the outcomes of the FCM simulation executed on the server-side are presented in a user-friendly visualisation. There is also an integrated console, which displays useful information regarding the execution of the corresponding iterative FCM simulation (e.g., warnings, FCM layout information, etc.).

The main contribution of the In-Cognitive web application is the implementation of the methodology of selecting parameter λ as presented in this paper (Sects. 3 and 4). To our knowledge, all FCM software tools (e.g., Mohr 1997; Margaritis et al. 2002; Aguilar and Contreras 2010; Papaioannou et al. 2010; Cheah et al. 2011; Gray et al. 2013; De Franciscis 2014; Poczęta et al. 2015; Nápoles et al. 2017; Nikas et al. 2017, 2019; Tsadiras et al. 2021) do not contain any software module to select λ based on the FCM layout. Instead, parameter λ is considered a constant parameter usually equal to one (Nikas et al. 2019).

Table 1 Node descriptions

Node	Description	Operation
C1	B1. Ongoing economic recession	Input node
C2	B2. Poor public acceptance	Input node
C3	B3. Regulatory framework instability	Input node
C4	B4. High technological cost	Input node
C5	B5. Poor political prioritisation	Input node
C6	P1. Financial incentives for large-scale projects	Input node
C7	P2. Enhanced land-use planning	Input node
C8	P3. Wide-scale deployment of smart meters	Input node
C9	P4. Financial incentives for storage units and devices	Input node
C10	S1. Monitoring capacity for energy consumption	Intermediate node
C11	S2. Control of utility bills	Intermediate node
C12	S3. Privacy invasion concerns	Intermediate node
C13	S4. Demand flexibility	Intermediate node
C14	S5. Trust in institutions	Intermediate node
C15	S6. Development of large-scale solar projects	Intermediate node
C16	S7. Technological lock-ins	Intermediate node
C17	S8. Share of lignite in the energy mix	Intermediate node
C18	S9. Share of RES in the power generation mix	Intermediate node
C19	S10. Grid stability	Intermediate node
C20	S11. Wholesale electricity prices	Intermediate node
C21	S12. Energy security	Intermediate node
C22	S13. Coal mining jobs	Intermediate node
C23	S14. Small-scale energy storage	Intermediate node
C24	S15. 'Green' engineering and consulting jobs	Intermediate node
C25	S16. Not-In-My-Backyard complaints	Intermediate node
C26	C1. Electricity costs for end-users	Output node
C27	C2. Economic growth in the long-term	Output node
C28	C3. Investments	Output node
C29	C4. Employment	Output node
C30	C5. Tariff deficits	Output node

Table 2 Socio-economic risk scenarios

Node	Node values				
	Sustainability	Middle of the road	Regional rivalry	Inequality	Fossil-fuelled development
C1	− 0.5	0.1	− 0.2	0.6	− 0.7
C2	− 0.7	− 0.1	0.65	0.75	− 0.7
C3	− 0.8	− 0.1	0.6	0.8	− 0.8
C4	− 0.7	0.2	− 0.1	− 0.35	− 0.7
C5	− 0.6	0.2	0.6	0.9	0.15

Table 3 Policies and corresponding input nodes

Nodes	Policies			
	Policy 1 (P1)	Policy 2 (P2)	Policy 3 (P3)	Policy 4 (P4)
C6	1	0	0	0
C7	0	1	0	0
C8	0	0	1	0
C9	0	0	0	1

6 Case study validation of the proposed framework and software

There is a plethora of studies applying the FCM theory in energy/climate policy (e.g., Nikas and Doukas 2016; Nikas et al. 2018, 2019, 2020; Doukas and Nikas 2020). In Nikas et al. (2020), the authors proposed an FCM layout to identify the most pertinent implementation risks to the diffusion of new solar power before calculating the long-term socioeconomic impacts of wide-scale solar PV deployment in an energy system and macroeconomic analysis in Greece, building on the uncertainty space associated with the identified implementation risks.

Table 1 briefly describes each node/concept of the FCM, while Table 6 in the Appendix presents the FCM layout in tabular format. Nodes C_1 to C_9 are the steady nodes. Nodes C_1 to C_5 correspond to the barriers of solar-based energy transition in Greece as suggested by the stakeholders (uncertainty drivers). Nodes C_6 to C_9 correspond to various policies (policy drivers). C_{26} to C_{30} are the output nodes (concepts under examination) and C_{10} to C_{25} are the intermediate nodes that change their values through iterations. Various value combinations of C_1 to C_5 are illustrated in Table 2, representing different socio-economic risk scenarios—i.e., socioeconomic paths (SP), hereafter. We adapt the following abbreviations regarding the various SPs (see Table 2): SP1: Sustainability, SP2: Middle of the road, SP3: Regional rivalry, SP4: Inequality and SP5: Fossil fuelled development. For each SP, four policies, P_1, P_2, P_3 and P_4 (see Table 3) are applied to explore their effect on the output nodes. Therefore, the following input combinations are applied to the introduced FCM: SP1_P1 to SP1_P4, SP2_P1 to SP2_P4, SP3_P1 to SP3_P4, SP4_P1 to SP4_P4 and SP5_P1 to SP5_P4.

After applying the analysis of Sect. 4, the norms of matrix $\boldsymbol{W}^*$ of FCM layout of Table 6 are:

$$\|\boldsymbol{W}\|_F^* \approx 1.522, \tag{34}$$

$$\|\mathbf{W}\|_\infty^* \approx 2.708 \tag{35}$$

and

$$\|\mathbf{W}\|_s^* \approx 1.421. \tag{36}$$

From Eqs. (30) to (33)

$$\lambda_s' = \frac{4}{\|\boldsymbol{W}\|_F^*} = \frac{4}{1.522} \approx 2.628, \tag{37}$$

$$\lambda_h' = \frac{1}{\|\boldsymbol{W}\|_F} = \frac{1}{1.522} \approx 0.657, \tag{38}$$

$$\lambda_s^* = \frac{1.317}{\|\mathbf{W}\|_s^*} = \frac{1.317}{1.421} \approx 0.927, \tag{39}$$

$$\lambda_h^* = \frac{1.14}{\|\mathbf{W}\|_\infty^*} = \frac{1.14}{2.708} \approx 0.421. \tag{40}$$

Finally, from Eqs. (21) and (22)

$$\lambda_s < min(2.628, 0.927) = 0.927 \tag{41}$$

and

$$\lambda_h < min(0.657, 0.421) = 0.421. \tag{42}$$

In this example the smallest bounds for both λ_s and λ_h are equal to the proposed ones (see Sect. 3.3.2).

All simulations are performed and visualised in the "In-Cognitive" software application in the sub-sections below. In Sect. 6.1, we illustrate the results of FCM simulations for S2_P3 (S2: Middle of the road, P3: Wide-scale deployment of smart meters) when the FCM is equipped with hyperbolic tangent transfer function. The values of parameters λ vary so that we can reach to useful conclusion regarding the analysis of Sects. 3 and 4 (we include the proposed bound $\lambda_h = 0.421$ as well). Moreover, the final concept values, A_i^k, is not normalised so that we can compare the results for various λ values. The normalisation procedure described in Sects. 3.4 and 4.2 is only applied to lambdas smaller than the proposed bounds, λ_s^* and λ_h^*. In contrast, the normalisation procedure and the proposed $\lambda_h = 0.421$ are only applied in Sect. 6.2.

6.1 Hyperbolic tangent FCM for different parameter λ values

Figures 8, 9, 10, 11 and 12 present the distributions of arguments x_i^k's of Eq. (8) for all intermediate and output nodes through all iterations. For all $\lambda_h \leq 0.421$ the arguments do not exceed the turning points (Figs. 8, 9); the arguments always lie in the almost-linear region. For $\lambda = 1$ (Fig. 10), a commonly used value in FCM simulations, the arguments are already out of the turning points and the A_i^k's values have distortion due to the curved regions of the transfer function. We also observe that the greater the lambda parameter, the more arguments fall within the tails of the transfer function; consequently more A_i^k receive

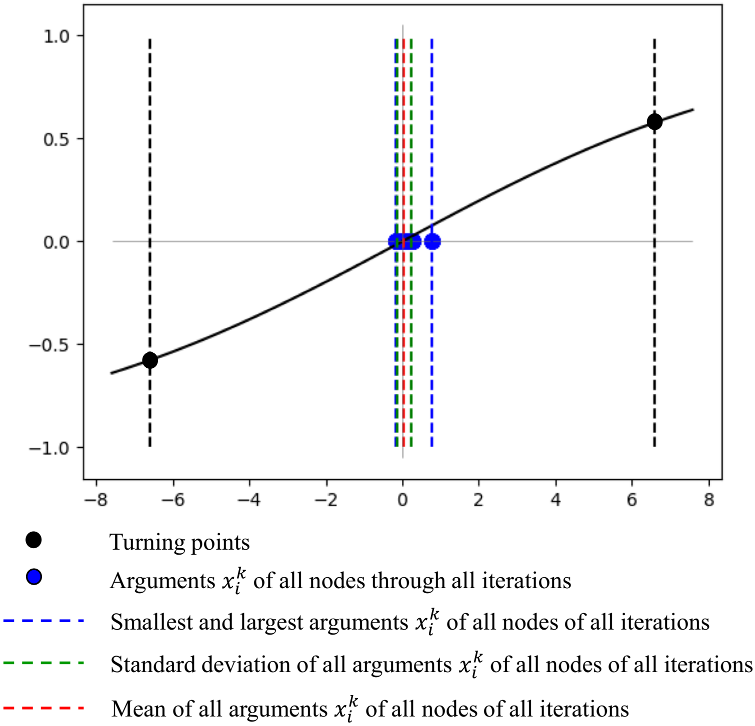

Fig. 8 Hyperbolic tangent FCM with λ = 0.1, SP: middle of the road, policy: P3 (SP2_P3)

±1 value (see Figs. 11, 12). Due to this effect, the final output vector is dense around the ±1 region, making the inferences ambiguous (see Table 4 for $\lambda = 10$ to $\lambda = 100$). This observation is in accordance with the analysis in Sect. 3.2 where we concluded that the greater the lambda parameter ($\lambda \to \infty$), the closer to the step function the transfer function gets, and the final node values get close to ±1 (undesired condition). In this specific application, for $\lambda_h > \lambda'_h = 0.657$ (i.e., Table 4 for $\lambda = 1$ to $\lambda = 100$) the FCM concludes to a fixed-point despite, according to Axelrod et al. (2015), the existence of a fixed point not being guaranteed for $\lambda_h > \lambda'_h$. This means that, if we try different excitations (other than S2_P3), we may get chaotic FCM behaviour when $\lambda_h > \lambda'_h = 0.657$. Finally, it is worth pointing out that the ordering of final output values is different when λ varies (Table 5), as expected by the analysis in Sect. 3—the variation refers to the stage before normalisation.

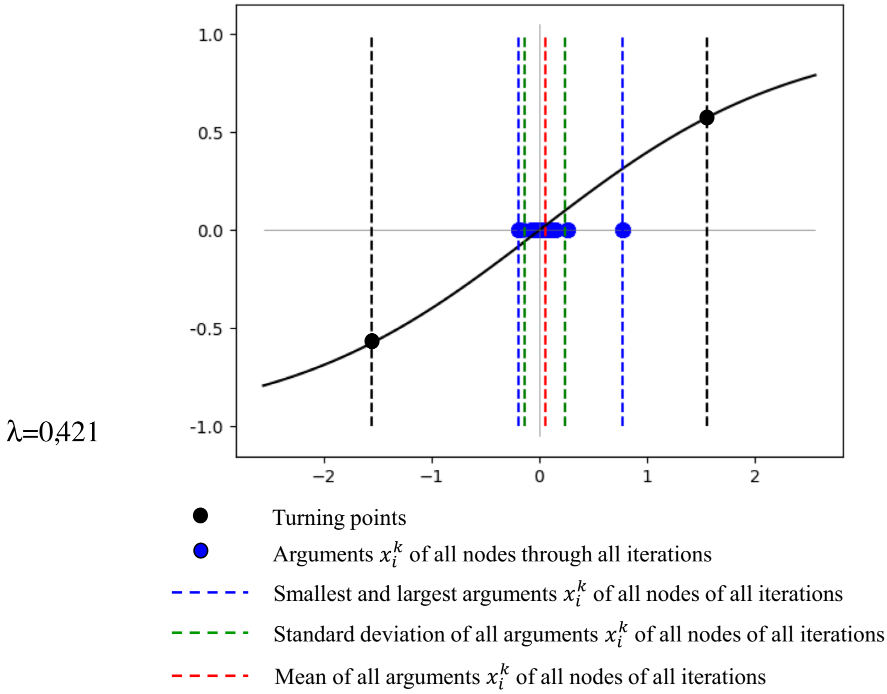

Fig. 9 Hyperbolic tangent FCM with λ = 0.421, SP: middle of the road, policy: P3 (SP2_P3)

6.2 Proposed parameter *λ* values with normalised final output vector

Figure 13 illustrates the values of all intermediate and output nodes during all iterations when the excitation is S2_P3 and $\lambda_h = 0.421$. All of them are normalised based on Eq. (26). The distribution of all arguments (Eq. (8)) through all iterations are as in Fig. 9. We can see that, for all x_i^k and their corresponding A_i^k values, the almost linear region is much larger. This happens due to the given SP2_P3 excitation. Different excitation would yield different distribution of x_i^k values but all these distributions would fall within the almost linear region because $\lambda_h = 0.421 < \lambda_h^* \approx 0.4211$. Finally, it should be noted that values do not fall within a narrow band region and therefore their ordering is clear and closer to a realistic representation of relative values of each node's deviation. This happens because, in the almost linear region, the deviations of A_i^k values are proportional to the deviations of x_i^k values (see Sect. 3.2).

7 Remarks and conclusions

We have proposed a framework for identifying a value for parameter λ for both log-sigmoid and hyperbolic tangent FCM transfer functions. With the previous state-of-the-art λ values, the transfer function was active for all possible f values. Given that both transfer functions have a curved region close to their tails (see Fig. 4) thereby

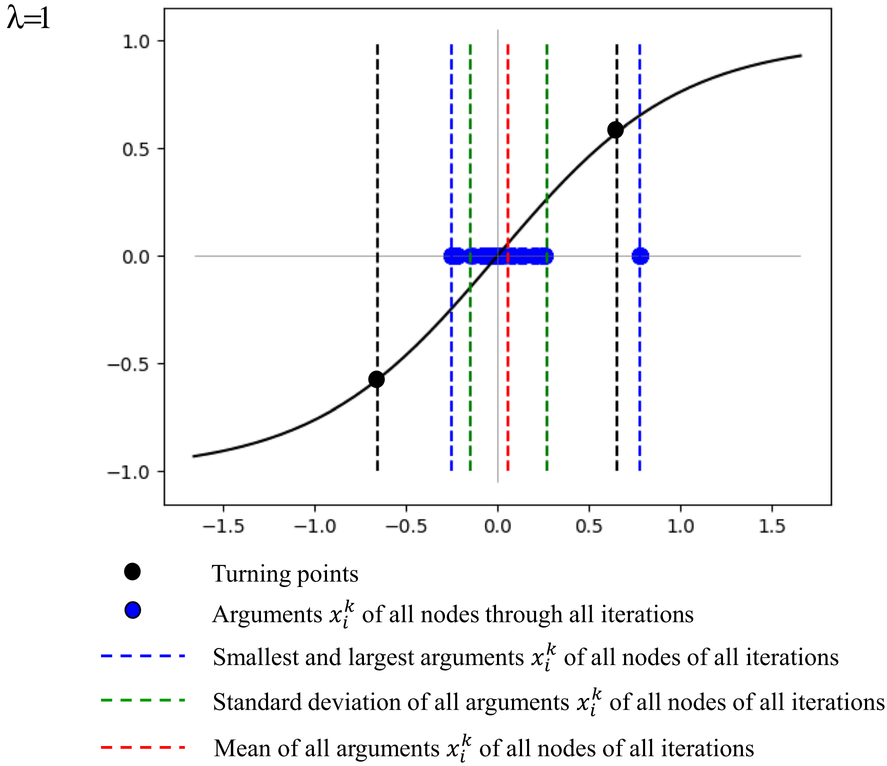

Fig. 10 Hyperbolic tangent FCM with λ = 1, SP: middle of the road, policy: P3 (SP2_P3)

creating distortion, final node values usually concluded to an overcrowded region (close to 0 and 1 or ±1, respectively), hence unclear inference. To tackle this barrier, we proposed that transfer functions should operate in the almost linear region (see Fig. 4). The latter requirement yielded a certain bound for parameter λ. We also demonstrated why parameter λ should not be excessively large or small (see Sect. 3.2). Therefore, we reached the conclusion that parameter λ must be as close to the proposed bounds in Eqs. (21) and (22). The analysis was performed for FCMs with or without steady nodes. We also proposed a normalisation procedure so that outcomes are clear, distinct, and sufficient for inferences.

Based on the proposed methodology, we furthermore developed a web software application written in Python, called "In-Cognitive", containing a user-friendly GUI that allows non-expert users to connect to the server, define the FCM layout (e.g., nodes, their weight interconnection, input state vector if any, etc.) and then request the results. The choice of parameter λ is taken endogenously based on Sects. 3 and 4.

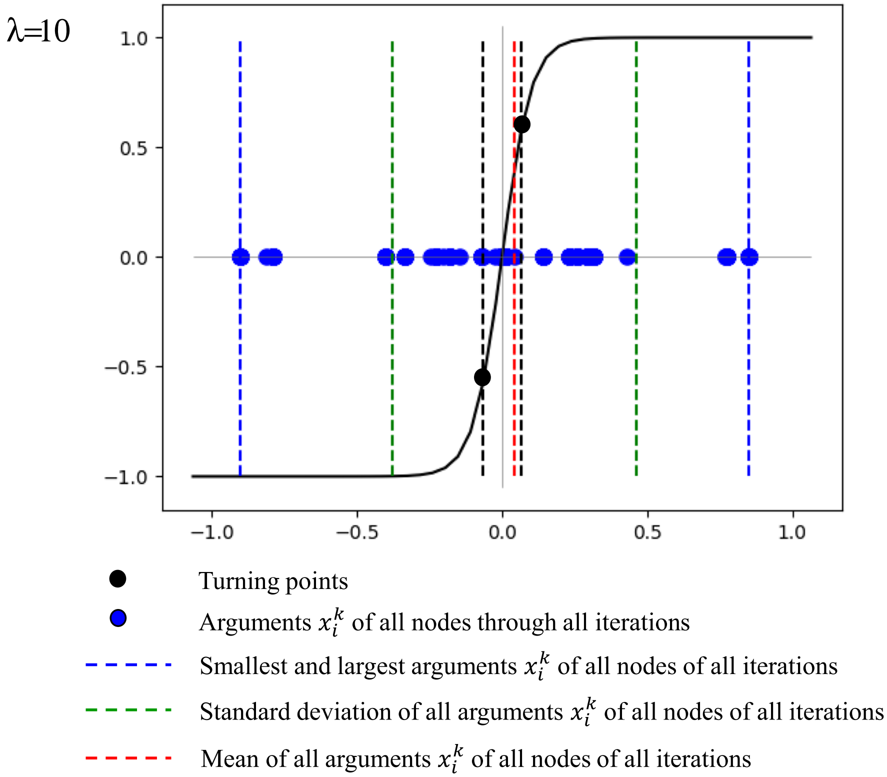

Fig. 11 Hyperbolic tangent FCM with λ = 10, SP: middle of the road, policy: P3 (SP2_P3)

Finally, by using the "In-Cognitive" software application, we ran a simulation of an FCM layout drawn from a real-world application in the literature (Nikas et al. 2020), validating the methodological takeaways of Sects. 3 and 4.

The parameter λ bounds that are proposed in this research aim to contribute to the hitherto ambiguity of FCM implementation and results, since different parameters λ yield different FCM outcomes and therefore different inferences. By providing an objective criterion to select a unique parameter λ we hope to contribute to further exploitation of FCM theory in research and policy-/decision-making.

A caveat of this study is that it focuses on a parameter of the transfer function that is defined by the analyst. On one hand, this means that other parameters

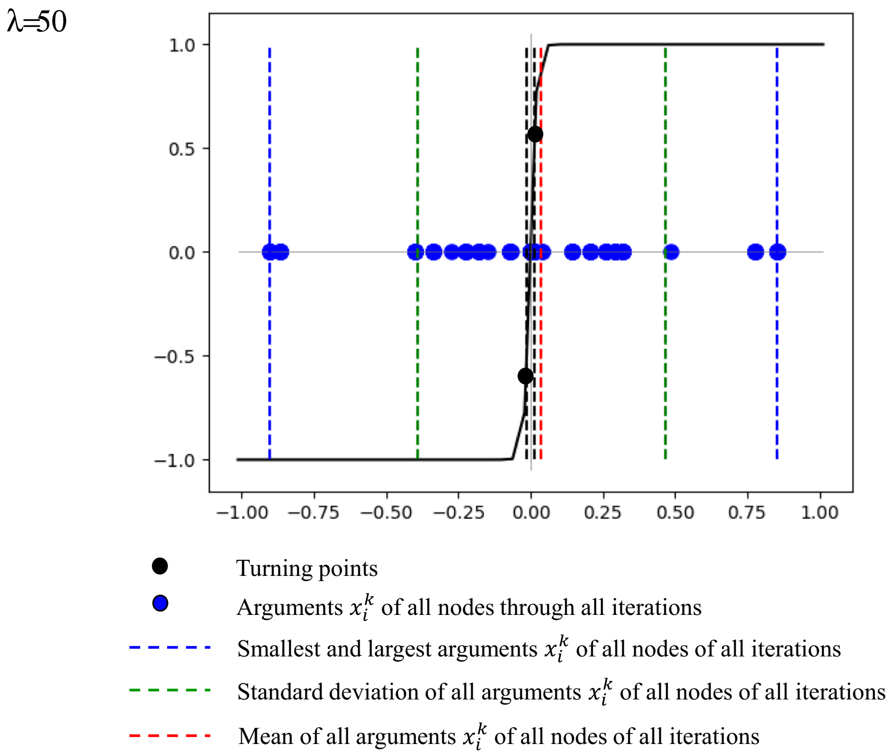

Fig. 12 Hyperbolic tangent FCM with λ = 50, SP: middle of the road, policy: P3 (SP2_P3)

Table 4 FCM output node values for different parameters λ

Node	Node final values					
	λ = 0.1	λ = 0.421	λ = 1	λ = 10	λ = 50	λ = 100
Output nodes						
C26	− 9.9313E−05	− 0.00717	− 0.08205	− 0.99934	− 1	− 1
C27	0	0	0	0	0	0
C28	− 2.4574E−04	0.00356	0.07818	0.98154	1	1
C29	0	0	0	0	0	0
C30	1.3504E−03	0.02886	0.20616	1.00000	1	1

Table 5 Ordering of FCM output node values for different parameters λ

Nodes/concepts					
$\lambda=0.1$	$\lambda=0.421$	$\lambda=1$	$\lambda=10$	$\lambda=50$	$\lambda=100$
Ascending ordering					
C28	C26	C26	C26	C26	C26
C26	C27	C27	C27	C27	C27
C27	C29	C29	C29	C29	C29
C29	C28	C28	C28	C28	C28
C30	C30	C30	C30	C30	C30

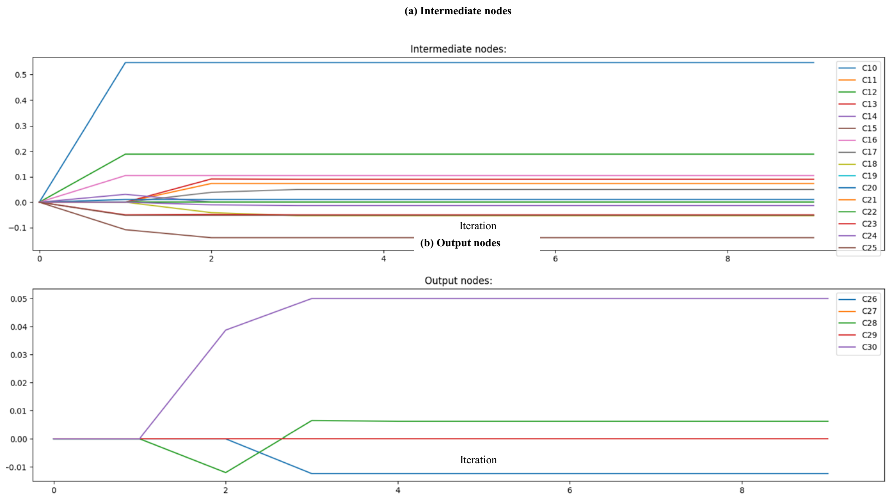

Fig. 13 All iterations of hyperbolic tangent FCM with λ = 0.421 and normalised final values, SP: middle of the road, policy: P3 (SP2_P3)

defined by the analyst have not been touched. For example, as a prospect of our research, the impact of the choice of transfer function (among sigmoid and hyperbolic tangent) on the robustness of the inference/results must be thoroughly examined. This also applies for parameter d_i of the driver function (Eq. 2) and the extent to which it can retain its physical meaning in the FCM model simulation. On the other hand, this caveat also means that the impact of aspects of the FCM model that are (largely) defined by the decision-makers, such as the FCM layout and the weight matrix, must also be further explored. On the latter, much research has been carried out in the form of learning algorithms; however, the extent to which the simulation outcomes change with regard to input data uncertainty (e.g., via Monte Carlo analysis in the weight matrix) is largely understudied. Future research should finally focus on improving the proposed normalisation procedure, which squashes node values to a smaller range based on the presented example, thereby rendering differences within the final state vector less distinct and therefore any conclusion harder.

Appendix

See Table 6.

Table 6 Weight node interconnections

Nodes		Weight	Nodes		Weight
Source	Target		Source	Target	
C1	C15	– 0.442	C14	C13	0.097
C1	C20	– 0.375	C14	C23	0.11
C1	C23	– 0.348	C15	C17	– 0.852
C2	C12	0.594	C15	C18	0.902
C2	C25	0.706	C15	C24	0.226
C3	C14	– 0.421	C15	C30	– 0.852
C3	C16	– 0.132	C16	C15	– 0.719
C3	C23	– 0.245	C16	C28	– 0.274
C4	C15	– 0.52	C17	C21	0.722
C4	C20	0.261	C17	C22	0.888
C4	C23	– 0.29	C18	C19	– 0.521
C5	C16	0.651	C19	C20	– 0.311
C6	C15	0.487	C20	C26	– 0.932
C7	C15	0.229	C20	C28	– 0.419
C8	C10	0.776	C21	C27	0.322
C8	C12	0.319	C22	C29	0.21
C9	C23	0.792	C23	C19	0.9
C10	C11	0.319	C23	C24	0.189
C10	C13	0.391	C24	C29	0.196
C11	C26	– 0.402	C25	C15	– 0.311
C12	C14	– 0.381	C28	C27	0.481
C13	C28	0.481	C29	C27	0.378

Acknowledgements The most important part of this research is based on the H2020 European Commission Project "PARIS REINFORCE" under Grant Agreement No. 820846. The sole responsibility for the content of this paper lies with the authors. The paper does not necessarily reflect the opinion of the European Commission.

Funding European Commission Horizon 2020 Framework, 'PARIS REINFORCE' Research and Innovation Project, Grant Agreement No. 820846.

Availability of data and materials Data used in the case study is available from Nikas, A., Stavrakas, V., Arsenopoulos, A., Doukas, H., Antosiewicz, M., Witajewski-Baltvilks, J., & Flamos, A. (2020). Barriers to and consequences of a solar-based energy transition in Greece. *Environmental Innovation and Societal Transitions, 35*, 383–399.

Code availability The code of the *In-Cognitive* software is open source and available on Github https://github.com/ThemisKoutsellis/InCognitive.

Declarations

Conflict of interests The authors declare that they have no conflict of interests.

References

Abbaspour Onari M, Jahangoshai Rezaee M (2020) A fuzzy cognitive map based on Nash bargaining game for supplier selection problem: a case study on auto parts industry. Oper Res. https://doi.org/10.1007/s12351-020-00606-1

Aguilar J, Contreras J (2010) The FCM designer tool. In: Glikas M (ed) Fuzzy cognitive maps: advances in theory, methodologies, tools and applications. Springer, Berlin, pp 71–88

Amer M, Daim TU, Jetter A (2016) Technology roadmap through fuzzy cognitive map-based scenarios: the case of wind energy sector of a developing country. Technol Anal Strateg Manag 28:131–155

Amirkhani A, Papageorgiou EI, Mohseni A, Mosavi MR (2017) A review of fuzzy cognitive maps in medicine: taxonomy, methods, and applications. Comput Methods Programs Biomed 142:129–145

Amirkhani A, Papageorgiou EI, Mosavi MR, Mohammadi K (2018) A novel medical decision support system based on fuzzy cognitive maps enhanced by intuitive and learning capabilities for modeling uncertainty. Appl Math Comput 337:562–582

Antosiewicz M, Nikas A, Szpor A et al (2020) Pathways for the transition of the Polish power sector and associated risks. Environ Innov Soc Transit 35:271–291

Apostolopoulos ID, Groumpos PP, Apostolopoulos DI (2017) A medical decision support system for the prediction of the coronary artery disease using fuzzy cognitive maps. In: Conference on creativity in intelligent technologies and data science. Springer, pp 269–283

Axelrod R (2015) Structure of decision: the cognitive maps of political elites. Princeton University Press, Princeton

Azevedo ARSC, Ferreira FAF (2019) Analyzing the dynamics behind ethical banking practices using fuzzy cognitive mapping. Oper Res 19:679–700. https://doi.org/10.1007/s12351-017-0333-6
Bevilacqua M, Ciarapica FE, Mazzuto G (2018) Fuzzy cognitive maps for adverse drug event risk management. Saf Sci 102:194–210
Boutalis Y, Kottas T, Christodoulou M (2008) On the existence and uniqueness of solutions for the concept values in fuzzy cognitive maps. In: 2008 47th IEEE conference on decision and control. IEEE, pp 98–104
Cakmak EH, Dudu H, Eruygur O et al (2013) Participatory fuzzy cognitive mapping analysis to evaluate the future of water in the Seyhan Basin. J Water Clim Change 4:131–145
Carvalho JP, Tomé JAB (2004) Qualitative modelling of an economic system using rule-based fuzzy cognitive maps. In: 2004 IEEE international conference on fuzzy systems (IEEE Cat. No. 04CH37542). IEEE, pp 659–664
Ceccato L (2012) Three essays on participatory processes and integrated water resource management in developing countries. Università Ca' Foscari Venezia, Venice
Çelik FD, Ozesmi U, Akdogan A (2005) Participatory ecosystem management planning at Tuzla lake (Turkey) using fuzzy cognitive mapping. arXiv Prepr q-bio/0510015
Cheah WP, Kim YS, Kim KY, Yang HJ (2011) Systematic causal knowledge acquisition using FCM constructor for product design decision support. Expert Syst Appl 38:15316–15331. https://doi.org/10.1016/j.eswa.2011.06.032
Craiger P, Coovert MD (1994) Modeling dynamic social and psychological processes with fuzzy cognitive maps. In: Proceedings of 1994 IEEE 3rd international fuzzy systems conference. IEEE, pp 1873–1877
de Franciscis D (2014) JFCM: a Java library for fuzzy cognitive maps. In: Papageorgiou EI (ed) Fuzzy cognitive maps for applied sciences and engineering. Springer, Berlin, pp 199–220
Doukas H, Nikas A (2020) Decision support models in climate policy. Eur J Oper Res 280:1–24. https://doi.org/10.1016/j.ejor.2019.01.017
Felix G, Nápoles G, Falcon R et al (2019) A review on methods and software for fuzzy cognitive maps. Artif Intell Rev 52:1707–1737. https://doi.org/10.1007/s10462-017-9575-1
Fons S, Achari G, Ross T (2004) A fuzzy cognitive mapping analysis of the impacts of an eco-industrial park. J Intell Fuzzy Syst 15:75–88
Froelich W, Papageorgiou EI, Samarinas M, Skriapas K (2012) Application of evolutionary fuzzy cognitive maps to the long-term prediction of prostate cancer. Appl Soft Comput 12:3810–3817
Georgopoulos VC, Malandraki GA, Stylios CD (2003) A fuzzy cognitive map approach to differential diagnosis of specific language impairment. Artif Intell Med 29:261–278
Ghaderi SF, Azadeh A, Nokhandan BP, Fathi E (2012) Behavioral simulation and optimization of generation companies in electricity markets by fuzzy cognitive map. Expert Syst Appl 39:4635–4646
Gray SA, Gray S, Cox LJ, Henly-Shepard S (2013) Mental modeler: a fuzzy-logic cognitive mapping modeling tool for adaptive environmental management. In: 2013 46th Hawaii international conference on system sciences. IEEE, pp 965–973
Gray SRJ, Gagnon AS, Gray SA et al (2014) Are coastal managers detecting the problem? Assessing stakeholder perception of climate vulnerability using fuzzy cognitive mapping. Ocean Coast Manag 94:74–89
Harmati IÁ, Hatwágner MF, Kóczy LT (2018) On the existence and uniqueness of fixed points of fuzzy cognitive maps. In: international conference on information processing and management of uncertainty in knowledge-based systems. Springer, pp 490–500
Harmati IÁ, Kóczy LT (2018) On the existence and uniqueness of fixed points of fuzzy set valued sigmoid fuzzy cognitive maps. In: 2018 IEEE international conference on fuzzy systems (FUZZ-IEEE). IEEE, pp 1–7
Hobbs BF, Ludsin SA, Knight RL et al (2002) Fuzzy cognitive mapping as a tool to define management objectives for complex ecosystems. Ecol Appl 12:1548–1565
Hsueh S-L (2015) Assessing the effectiveness of community-promoted environmental protection policy by using a Delphi-fuzzy method: a case study on solar power and plain afforestation in Taiwan. Renew Sustain Energy Rev 49:1286–1295
Huang S-C, Lo S-L, Lin Y-C (2013) Application of a fuzzy cognitive map based on a structural equation model for the identification of limitations to the development of wind power. Energy Policy 63:851–861

Karavas C-S, Kyriakarakos G, Arvanitis KG, Papadakis G (2015) A multi-agent decentralized energy management system based on distributed intelligence for the design and control of autonomous polygeneration microgrids. Energy Convers Manag 103:166–179

Knight CJK, Lloyd DJB, Penn AS (2014) Linear and sigmoidal fuzzy cognitive maps: an analysis of fixed points. Appl Soft Comput 15:193–202

Kok K (2009) The potential of fuzzy cognitive maps for semi-quantitative scenario development, with an example from Brazil. Glob Environ Change 19:122–133

Kosko B (1986) Fuzzy cognitive maps. Int J Man Mach Stud 24:65–75

Kottas TL, Boutalis YS, Christodoulou MA (2010) Fuzzy cognitive networks: adaptive network estimation and control paradigms. In: Glykas M (ed) Fuzzy cognitive maps. Springer, Berlin, pp 89–134

Koulouriotis DE (2004) Investment analysis & decision making in markets using adaptive fuzzy causal relationships. Oper Res 4:213–233. https://doi.org/10.1007/bf02943610

Koulouriotis DE, Diakoulakis IE, Emiris DM (2001) A fuzzy cognitive map-based stock market model: synthesis, analysis and experimental results. In: 10th IEEE international conference on fuzzy systems.(Cat. No. 01CH37297). IEEE, pp 465–468

Kyriakarakos G, Dounis AI, Arvanitis KG, Papadakis G (2012) A fuzzy cognitive maps–petri nets energy management system for autonomous polygeneration microgrids. Appl Soft Comput 12:3785–3797

Lee IK, Kwon SH (2010) Design of sigmoid activation functions for fuzzy cognitive maps via Lyapunov stability analysis. IEICE Trans Inf Syst 93:2883–2886

Liu Z-Q, Satur R (1999) Contextual fuzzy cognitive map for decision support in geographic information systems. IEEE Trans Fuzzy Syst 7:481–494

Margaritis M, Stylios C, Groumpos P (2002) Fuzzy cognitive map software. In: 10th international conference on software, telecommunications and computer networks SoftCom, pp 8–11

Markaki O, Askounis D (2021) Assessing the operational and economic efficiency benefits of dynamic manufacturing networks through fuzzy cognitive maps: a case study. Oper Res 21:925–950. https://doi.org/10.1007/s12351-019-00488-y

Mendoza GA, Prabhu R (2006) Participatory modeling and analysis for sustainable forest management: overview of soft system dynamics models and applications. For Policy Econ 9:179–196

Mohr S (1997) Software design for a fuzzy cognitive map modeling tool. Rensselaer Polytechnic Institute, Troy

Nápoles G, Leon Espinosa M, Grau I et al (2018) Fuzzy cognitive maps based models for pattern classification: advances and challenges BT—soft computing based optimization and decision models: to commemorate the 65th birthday of Professor José Luis "Curro" Verdegay. In: Cruz Corona C (ed) Pelta DA. Springer International Publishing, Cham, pp 83–98

Nápoles G, Leon M, Grau I, Vanhoof K (2017) Fuzzy cognitive maps tool for scenario analysis and pattern classification. In: 2017 IEEE 29th international conference on tools with artificial intelligence (ICTAI). IEEE, pp 644–651

Nikas A, Doukas H (2016) Developing robust climate policies: a fuzzy cognitive map approach. In: Doumpos M, Zopounidis C, Grigoroudis E (eds) Robustness analysis in decision aiding, optimization, and analytics. Springer, Cham, pp 239–263

Nikas A, Doukas H, Lieu J et al (2017) Managing stakeholder knowledge for the evaluation of innovation systems in the face of climate change. J Knowl Manag 21:1013–1034

Nikas A, Doukas H, van der Gaast W, Szendrei K (2018) Expert views on low-carbon transition strategies for the Dutch solar sector: a delay-based fuzzy cognitive mapping approach. IFAC-PapersOnLine 51:715–720. https://doi.org/10.1016/j.ifacol.2018.11.208

Nikas A, Ntanos E, Doukas H (2019) A semi-quantitative modelling application for assessing energy efficiency strategies. Appl Soft Comput 76:140–155

Nikas A, Stavrakas V, Arsenopoulos A et al (2020) Barriers to and consequences of a solar-based energy transition in Greece. Environ Innov Soc Transit 35:383–399

Olazabal M, Pascual U (2016) Use of fuzzy cognitive maps to study urban resilience and transformation. Environ Innov Soc Transit 18:18–40

Özesmi U, Özesmi SL (2004) Ecological models based on people's knowledge: a multi-step fuzzy cognitive mapping approach. Ecol Modell 176:43–64. https://doi.org/10.1016/j.ecolmodel.2003.10.027

Papaioannou M, Neocleous C, Sofokleous A, et al (2010) A generic tool for building fuzzy cognitive map systems. In: IFIP international conference on artificial intelligence applications and innovations. Springer, pp 45–52

Papakostas G, Boutalis Y, Koulouriotis D, Mertzios B (2006) A first study of pattern classification using fuzzy cognitive maps. In: International conference on systems, signals and image processing-INS-SIP. pp 369–374
Papakostas GA, Boutalis YS, Koulouriotis DE, Mertzios BG (2008) Fuzzy cognitive maps for pattern recognition applications. Int J Pattern Recognit Artif Intell 22:1461–1486
Penn AS, Knight CJK, Lloyd DJB et al (2013) Participatory development and analysis of a fuzzy cognitive map of the establishment of a bio-based economy in the Humber region. PLoS ONE 8:e78319
Poczęta K, Yastrebov A, Papageorgiou EI (2015) Learning fuzzy cognitive maps using structure optimization genetic algorithm. In: 2015 federated conference on computer science and information systems (FedCSIS). IEEE, pp 547–554
Puerto E, Aguilar J, López C, Chávez D (2019) Using multilayer fuzzy cognitive maps to diagnose autism spectrum disorder. Appl Soft Comput 75:58–71
Reckien D (2014) Weather extremes and street life in India—implications of fuzzy cognitive mapping as a new tool for semi-quantitative impact assessment and ranking of adaptation measures. Glob Environ Change 26:1–13
Satur R, Liu Z-Q (1999a) A contextual fuzzy cognitive map framework for geographic information systems. IEEE Trans Fuzzy Syst 7:481–494. https://doi.org/10.1109/91.797974
Satur R, Liu Z-Q (1999b) Contextual fuzzy cognitive maps for geographic information systems. In: FUZZ-IEEE'99. 1999b IEEE international fuzzy systems. conference proceedings (Cat. No. 99CH36315). IEEE, pp 1165–1169
Silva PC (1995) Fuzzy cognitive maps over possible worlds. In: Proceedings of 1995 IEEE international conference on fuzzy systems. IEEE, pp 555–560
Soler LS, Kok K, Camara G, Veldkamp A (2012) Using fuzzy cognitive maps to describe current system dynamics and develop land cover scenarios: a case study in the Brazilian Amazon. J Land Use Sci 7:149–175
Stach W, Kurgan LA, Pedrycz W (2008) Numerical and linguistic prediction of time series with the use of fuzzy cognitive maps. IEEE Trans Fuzzy Syst 16:61–72
Stylios CD, Groumpos PP (2004) Modeling complex systems using fuzzy cognitive maps. IEEE Trans Syst Man Cybern A Syst Hum 34:155–162
Tsadiras A, Pempetzoglou M, Viktoratos I (2021) Making predictions of global warming impacts using a semantic web tool that simulates fuzzy cognitive maps. Comput Econ 58:715–745. https://doi.org/10.1007/s10614-020-10025-1
Tsadiras AK (2008) Comparing the inference capabilities of binary, trivalent and sigmoid fuzzy cognitive maps. Inf Sci (NY) 178:3880–3894. https://doi.org/10.1016/j.ins.2008.05.015
Tsadiras AK, Kouskouvelis I (2005) Using fuzzy cognitive maps as a decision support system for political decisions: the case of Turkey's Integration into the European Union. In: Lecture notes in computer science, pp 371–381
van Vliet M, Kok K, Veldkamp T (2010) Linking stakeholders and modellers in scenario studies: the use of fuzzy cognitive maps as a communication and learning tool. Futures 42:1–14. https://doi.org/10.1016/j.futures.2009.08.005
Xirogiannis G, Stefanou J, Glykas M (2004) A fuzzy cognitive map approach to support urban design. Expert Syst Appl 26:257–268
Zhang W-R, Chen S-S, Bezdek JC (1989) Pool2: A generic system for cognitive map development and decision analysis. IEEE Trans Syst Man Cybern 19:31–39
Zhang W-R, Chen S-S, Wang W, King RS (1992) A cognitive-map-based approach to the coordination of distributed cooperative agents. IEEE Trans Syst Man Cybern 22:103–114